Solvation Dynamics of the Excited 1,2-(*p*-Cyano-*p*′-Methoxydiphenyl)-Ethyne†

Naoto Tamai,‡ Tateo Nomoto,§ Fumio Tanaka,*,|| Yoshinori Hirata,⊥,# and Tadashi Okada⊥

Department of Chemistry, School of Science, Kwansei Gakuin University, 2-1 Gakuen Sanda 669-1337, Japan, Faculty of Education, Mie University, 1515 Kamihama, Tsu 514-0008, Japan, Mie Prefectural College of Nursing, 1-1-1 Yumegaoka, Tsu 514-0116, Japan, and Department of Chemistry, Graduate School of Engineering Science, Osaka University, Toyonaka 560-8531, Japan

Received: July 3, 2001; In Final Form: December 31, 2001

Solvation dynamics of 1,2-(*p*-cyano-*p*′-methoxydiphenyl)-ethyne (CMPE) in various solvents were investigated by observing its time-resolved fluorescence and transient absorption in the picosecond regime. Anisotropy decays of CMPE in most of the solvents examined were apparently single-exponential, except for *n*-butanol, in which the decay was nonexponential. Dipole moment of CMPE in the excited state (μ_e), limiting anisotropy (A_0) and rotational diffusion coefficient (D_0) were obtained from the anisotropy decays with the theoretical expression based on continuum model combined with a nonlinear least-squares's method. The values of μ_e were linearly dependent on the solvent polarity except for benzene (9.9 D), and were 3.4 D in diethyl ether, 5.7 D in tetrahydrofuran, 13 D in *n*-butanol, 17 D in acetonitrile and 42 D in dimethyl sulfoxide. From transient absorption spectral measurements, it was demonstrated that the CT states appeared with time less than 10 ps in acetonitrile, 10 ps in methanol and 20 ps in dioxane after pulsed excitation, but not in *n*-hexane. These results reveal that the dipole moment of CMPE in the excited state is dependent on the solvent polarity. The values of D_0 in benzene and in polar solvents with short relaxation times were always less than those calculated with stick or slip model, which suggests that rotational volume of the excited CMPE increased by the solvation. Time-resolved Stokes shift and anisotropy of the fluorescence of CMPE in *n*-butanol were simultaneously analyzed to obtain $\mu_e = 14$ D, μ_g (the dipole moment in the ground state) $= 1.5$ D and $D_0 = 0.94$ ns^{-1}.

Introduction

A number of works have been reported on the solvation dynamics of excited polar molecules observed by means of time-resolved fluorescence Stokes shift.[1−5] Since Kivelson and Spears[6] emphasized the importance of dielectric friction on the anisotropy decay of aromatic ions, a number of works of time-resolved fluorescence anisotropy of polar molecules have been also reported.[7−16] Theoretical works of time-resolved Stokes shift for excited molecules were given by Bagchi et al.[17] and van der Zwan and Hynes[18] on the basis of continuum model. In these works, however, anisotropy decays and Stokes shift have been investigated independently.

Recently, we have reported an unified theory of both the Stokes shift and anisotropy decay based on continuum model.[19] In this work, we have investigated on the solvation dynamics of a rodlike molecule of 1,2-(*p*-cyano-*p*′-methoxydiphenyl)-ethyne (CMPE) in various solvents utilizing time-resolved fluorescence and transient absorption spectroscopy in the picosecond regime. The observed anisotropy decays and Stokes shift were analyzed with the unified theory.[19]

Experimental Section

CMPE was synthesized according to the method described elsewhere,[20] and purified in the mixed solvents of acetonitrile-water by a HPLC. Organic solvents were all spectral grade (Nacalai Tesque, Kyoto), and used without further purification. Corrected fluorescence spectra were measured with a spectrofluorometer (JASCO FP-770, Japan). Time-resolved fluorescence was measured with a synchronously pumped, cavity-dumped dye laser and a picosecond time-correlated single-photon counting apparatus.[21] Typical time width of the instrumental response function was 30 ps, whereas current pulse width of the dye laser was less than 10 ps. Sample solution was excited through a polarizer adjusted to a magic angle (54.7°). Observed decay curves of CMPE fluorescence were fit with a multiexponential functions as shown in eq 1, with a nonlinear least-squares's iterative convolution method based on Marquardt algorithm

$$F(t) = \sum_{i=1}^{N} \alpha_i \exp(-t/\tau_i) \tag{1}$$

The values of fluorescence anisotropy were calculated with polarized intensities of parallel $I_V(t)$ and perpendicular $I_H(t)$ to the polarized laser light, according to eq 2

$$A(t) = \frac{I_V(t) - I_H(t)}{I_V(t) + 2I_H(t)} \tag{2}$$

Time-resolved fluorescence spectra of CMPE were constructed from the observed decay curves at 400 different

† Part of the special issue "Noboru Mataga Festschrift".

* To whom correspondence should be addressed.

‡ Department of Chemistry, School of Science, Kwansei Gakuin University, 2-1 Gakuen Sanda 669-1337, Japan. (tamai@ksc.kwansei.ac.jp).

§ Faculty of Education, Mie University, 1515 Kamihama, Tsu 514-0008, Japan. (nomoto@edu.mie-u.ac.jp).

|| Mie Prefectural College of Nursing, 1-1-1 Yumegaoka, Tsu 514-0116, Japan. (fumio.tanaka@mcn.ac.jp).

⊥ Department of Chemistry, Graduate School of Engineering Science, Osaka University, Toyonaka 560-8531, Japan. (okada@chem.es.osaka-u.ac.jp).

Present address: Department of Materials Science, Faculty of Science, Kanagawa University, 2946 Tsuchiya, Hiratsuka 259-1293, Japan. (hirata@chem.kanagawa-u.ac.jp).

10.1021/jp0125092 CCC: $22.00
Published on Web 02/14/2002

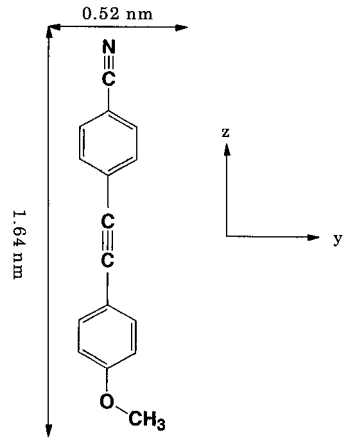

Figure 1. CMPE and molecular axes.

wavelengths. The spectra were corrected for the wavelength-dependent sensitivity of the detector system with a standard halogen lamp. The time-dependent Stokes shift was obtained by a set of the time-resolved fluorescence spectra.

The temperature of the samples for the measurements of the time-resolved fluorescence was controlled with circulating water.

Picosecond transient absorption spectra were measured by using a dye laser photolysis system pumped by second harmonics of a mode-locked Nd^{3+}:YAG laser (Quantel, Pico-chrome YG-503C/PTL-10). The details of the system were described elsewhere.[22] The sample was excited with second harmonics of Rhodamine-6G (295 nm) laser and a transient absorption spectrum between 380 and 980 nm was measured by using a picosecond white light generated in H_2O/D_2O mixture. Typically, the signal was averaged for 30 shots. To correct the transient absorption spectrum for the dispersion of the probe light, we measured optical Kerr effect of CCl_4 and determined the wavelength-dependent arrival times of the picosecond white light at the sample cell. The time resolution of this system was about 10 ps.

Method of Analyses. We have assumed CMDE as a prolate ellipsoid, and chosen the long axis of CMPE as *z*-axis (see Figure 1). We also assumed that the dipole moments in the excited and ground states, the transition moment of emission of CMPE are all along *z*-axis.

When a frequency-dependent dielectric constant is expressed with a single relaxation time, τ_D, the anisotropy decay is expressed by eq 3[19]

$$A(t) = \frac{1}{5}(3\cos\theta_g - 1)(A_2 e^{-a_2 t} + B_2 e^{-b_2 t}) \tag{3}$$

Here A_2, and B_2 can be obtained from eqs 4 and 5, respectively, with $r = 2$

$$A_r = \frac{a_r P_1 + (K_1 + P_0)}{(a_r - b_r)P_1} \tag{4}$$

$$B_r = -\frac{b_r P_1 + (K_1 + P_0)}{(a_r - b_r)P_1} \tag{5}$$

a_2 and b_2 are roosts of the following second-order polynomial

$$(i\omega)^2 - (i\omega)\left\{\frac{K_1 + P_0}{P_1} + r(r+1)\,D_0\right\} + \left(\frac{P_0}{P_1}\right)r(r+1)\,D_0 = 0 \tag{6}$$

D_0 is the rotational diffusion coefficient of solute molecule around short axes. The other constants appeared in above equations are given by eqs 7 to 9

$$K_1 = \frac{3\mu_e^2 A(1-A)(\epsilon_0 - \epsilon_\infty)}{ab^2\zeta_0}\left\{\frac{1 + (\epsilon_c - 1)A}{\epsilon_0 + (\epsilon_c - \epsilon_0)A}\right\} \tag{7}$$

$$P_0 = \frac{1}{\tau_D}\{\epsilon_0 + (\epsilon_c - \epsilon_0)A\} \tag{8}$$

$$P_1 = \epsilon_\infty + (\epsilon_c - \epsilon_\infty)A \tag{9}$$

Here, ϵ_0, ϵ_∞, and ϵ_c are static, optical and cavity's dielectric constants, respectively. *a* and *b* are half diameters of long and short axes of CMPE. *A* represents an extent of deviation of the molecular shape from a sphere.[23] The values of *a* and *b* for CMPE were evaluated to be 0.82 and 0.26 from CPK space-filling model, and then $A = 0.102$. μ_e is dipole moment of CMPE in the excited state. ζ_0 represents a mechanical friction and is related to D_0 by Einstein-Stokes equation, $D_0 = kT/\zeta_0$, where *k* and *T* are Boltzmann constant and temperature. Dielectric constant of cavity, ϵ_c, which is considered to be optical dielectric constant of solute,[23] is assumed to be 5.0. Changes in the best-fit parameters were examined by varying ϵ_c from 4 to 6. The parameters were not changed appreciably upon changing ϵ_c in this range.

The time-dependence of Stokes shift is obtained as in eq 10 when the single relaxation time, τ_D, is assumed for the dielectric constant[19]

$$\langle\Delta E(t)\rangle = -F_1\left[\frac{A_1}{u + a_1}\{\mu_e^2 - \mu_e\mu_g - (\mu_e - \mu_g)^2 e^{-(u+a_1)t}\} + \frac{B_1}{u + b_1}\{\mu_e^2 - \mu_e\mu_g - (\mu_e - \mu_g)^2\, e^{-(u+b_1)t}\}\right] \tag{10}$$

In eq 10, F_1 and *u* are given by eqs 11 and 12, respectively

$$F_1 = \frac{3A(1-A)(\epsilon_\infty - \epsilon_c)\{1 + (\epsilon_c - 1)A\}^2}{ab^2\tau_D\{\epsilon_\infty + (\epsilon_c - \epsilon_\infty)A\}^2} \tag{11}$$

$$u = \frac{\epsilon_0 + (\epsilon_c - \epsilon_0)A}{\tau_D\{\epsilon_\infty + (\epsilon_c - \epsilon_\infty)A\}} \tag{12}$$

A_1 and B_1 are obtained from eqs 4 and 5, respectively, with $r = 1$. a_1 and b_1 are also obtained from eq 6 at $r = 1$.

Frequency-dependent dielectric constant of *n*-propanol is expressed with three relaxation times and given below in eq 13[23,24]

$$\epsilon(\omega) = \epsilon_\infty + (\epsilon_0 - \epsilon_\infty)\sum_{j=1}^{3}\frac{g_j}{1 + i\omega\tau_j} \tag{13}$$

where

$$\sum_{j=1}^{3} g_j = 1 \tag{14}$$

The values of τ_j and g_j are given by Castner et al.[24] In the relevant case, the Stokes shift is represented with eq 15

$$\langle \Delta E(t) \rangle = -F_3 \sum_{j=1}^{4} \sum_{l=1}^{3} \frac{A_j B_l}{a_j + b_l} \{ \mu_e^2 - \mu_e \mu_g + (\mu_e - \mu_g)^2 e^{-(a_j + b_l)t} \} \quad (15)$$

where

$$F_3 = \frac{3A(1-A)(\epsilon_0 - \epsilon_\infty)\{1 + (\epsilon_c - 1)A\}}{ab^2 \epsilon_c \{\epsilon_\infty + (\epsilon_c - \epsilon_\infty)A\}} \quad (16)$$

The constants, A_j, B_l, a_j, and b_l ($j = 1$ to 4, and $l = 1$ to 3) may be obtained according to the method described in Appendix.

For the analyses of anisotropy decays, the dipole moment of the excited state, μ_e and an angle between transition moments of absorption and emission, θ_g were determined so as to obtain the minimum value of χ_A^2 according to a nonlinear least-squares method based on Marquardt algorithm, at certain value of D_0. The least value of χ_A^2 was searched as D_0 was sequentially varied at a definite interval

$$\chi_A^2 = \frac{100}{N_A} \sum_{j=1}^{N_A} \frac{\{A_{calc}(t_j) - A_{obs}(t_j)\}^2}{A_{obs}(t_j)} \quad (17)$$

where N_A is number of data point in anisotropy decay and 100 is a weighed factor.

For the Stokes shift, $S(t) = \langle \Delta E(t) \rangle - \langle \Delta E(\infty) \rangle$ was analyzed. μ_e and μ_g were determined so as to obtain the minimum value of χ_S^2, at certain value of D_0 as in the analyses of anisotropy decays

$$\chi_S^2 = \frac{1000}{N_S} \sum_{j=1}^{N_S} \frac{\{S_{calc}(t_j) - S_{obs}(t_j)\}^2}{S_{obs}(t_j)} \quad (18)$$

where N_S is number of data point of Stokes shift and 1000 is a weighed factor, which is larger than the one of anisotropy, because N_S was much smaller than N_A. The best fit parameters of μ_e, μ_g, and D_0 were obtained at the minimum value of χ_S^2.

In *n*-butanol anisotropy decay and Stokes shift were simultaneously analyzed. μ_e, μ_g, θ_g, and D_0 were determined in the similar way to the anisotropy or Stokes shift analysis, so as to obtain the minimum value of χ^2 in eq 19

$$\chi^2 = \chi_A^2 + \chi_S^2 \quad (19)$$

Results

Spectroscopic Characteristics of CMPE. CMPE is a polar molecule and expected to exhibit large solvent effects. Fluorescence spectra of CMPE in *n*-hexane and in acetonitrile are shown in Figure 2. Table 1 shows spectroscopic characteristics of CMPE in various solvents. Weighed center of the first absorption band (the value in parentheses of abs. λ_{max} in Table 1) shifted a little toward longer wavelength with increase of the solvent polarity, although the extent of the shift was very small. The wavelength at maximum intensity of fluorescence band greatly shifted toward longer wavelength with increase of the solvent polarity. Relative fluorescence quantum yield showed a tendency of decrease with increase of the solvent polarity, although it was exceptionally high in dimethyl sulfoxide. This might be attributed to high viscosity of dimethyl sulfoxide.

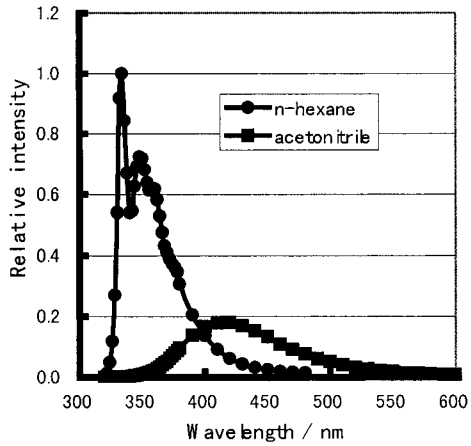

Figure 2. Fluorescence spectra of CMPE.

TABLE 1: Spectral Characteristics of CMPE

solvent	abs. λ_{max}/nm	ϵ_{max} ($\times 10^{-4}$)	em.[a] λ_{max}/nm	Q.Y.[b]
n-hexane	330 (310)[c]	4.1	334	0.21
	256	1.6	(356)[d]	
cyclohexane	333 (312)	4.2	338	0.23
	258	1.8	(360)	
dioxane	314 (312)	3.8	372	0.12
	260	2.0	(381)	
carbon tetrachloride	336 (314)	4.0	344	0.12
	260	2.0	(357)	
ethyl ether	312 (310)	3.5	370	0.057
	258	1.8	(378)	
tetrahydrofuran	315 (314)	3.8	385	0.077
	259	1.9	(397)	
dichloromethane	329	3.6	-	-
	260	1.7		
1,2-dichloroethane	329 (319)	3.7	-	-
	260	1.8		
2-methoxyethane	-	-	389	0.11
N.N-dimethylformamide	328	3.4	-	-
acetonitrile	324 (311)	3.7	418	0.091
	258	1.8	(425)	
dimethyl sulfoxide	329 (317)	3.4	421	0.16
	259	1.6	(431)	

[a] Excitation wavelength was 320 nm. [b] Relative quantum yields were determined by comparing the area of the corrected spectra with one of the standard (quinine bisulfate in 0.1 N H_2SO_4). [c] The values in parentheses indicate the inverse of the averaged wavenumbers over the first absorption bands. [d] The values in parentheses indicate the inverse of the averaged wavenumbers over the emission bands.

Rotational Diffusion Coefficient of CMPE in Non-Polar Solvents. CMPE is a rodlike molecule. Transition moments of both absorption and emission are considered to be along long axis of the molecule. Fluorescence anisotropy of CMPE decayed exponentially both in 2,2,4-trimethylpentane and in *n*-pentadecane. The values of limiting anisotropy, A_0, and rotational diffusion coefficient, D_0, were determined by the nonlinear least-squares's method as described in **Method of Analyses Section**. The obtained parameters are listed in Table 2. The values of D_0 were calculated with both stick model[25] and slip model.[26] The observed diffusion coefficient in 2,2,4-trimethylpentane was close to the calculated one with stick model, but in *n*-pentadecane to the one with slip model. Jiang and Blanchard[27] demonstrated that stick model was good enough for the rotational diffusion coefficient of perylene in nonpolar solvents with molecular size smaller than the solute molecule, whereas slip model was better for that of perylene in nonpolar solvents with molecular size larger than the solute molecule. They interpreted that the solute rotates together with solvent molecules

TABLE 2: Rotational Diffusion Coefficients of CMPE in Non-Polar Solvents[a]

solvent	η[b] (mPas)	D_0/ns^{-1} (obs)	(calc) slip model	D_0/ns^{-1} [c] stick model	A_0[d]
2,2,4-trimethyl-pentane	0.447	2.37	5.59	2.70	0.32
n-pentadecane	2.2	1.05	1.14	0.548	0.35

[a] The observed anisotropy was fit with the following equation: $A(t) = 1/5(3\cos\theta_g - 1)\exp(-6D_0t)$. The temperature was 30 °C. [b] Viscosity at 30 °C was evaluated from those of 2,2,4-trimethylpentane at 20 °C and *n*-pentadecane at 22 °C.[39] [c] The half diameters evaluated from CPK space-filling model are $a = 0.82$ nm and $b = 0.26$ nm. [d] A_0 is limiting polarization anisotropy. θ_g obtained by the best-fit procedure is related to A_0 by the equation, $A_0 = 1/5(3\cos\theta_g - 1)$

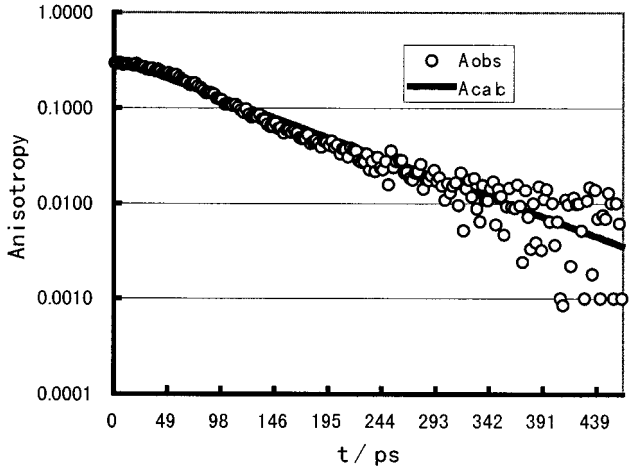

Figure 3. Anisotropy decay of CMPE in THF. Parameters used and calculated are listed in Table 3.

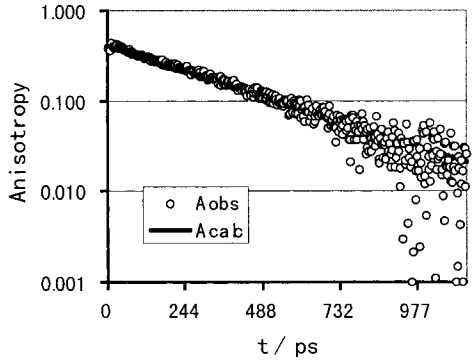

Figure 4. Anisotropy decay of CMPE in DMSO. Parameters used and calculated are listed in Table 3.

when molecular size of solute is larger than solvent molecules, whereas it rotates in the solvent molecules when molecular size of solute is smaller than solvent molecules. The present results are in accordance with their interpretation because CMPE is larger than 2,2,4-trimethylmethane, but smaller than *n*-pentadecane.

Anisotropy Decays in Polar Solvents and Dipole Moments of CMPE in the Excited State. Anisotropy decay of CMPE in tetrahydrofuran and in dimethyl sulfoxide is shown in Figure 3 and in Figure 4, respectively. The observed anisotropies are indicated with open circles. They decayed monoexponentially. These data were analyzed with the unified theory according to the method described previously. It is possible to determine the dipole moment of CMPE in the excited state directly from anisotropy decay, whereas only the difference between the dipole moments in the ground state and in the excited state is determined from Stokes shift. Used and obtained parameters are listed in Table 3. The μ_e of CMPE were obtained in various solvents at several temperatures and at different monitoring wavelengths. The values of μ_e did not change significantly upon changing temperature and emission wavelength. The values of μ_e were 9.9 ± 0.3 D in benzene, 3.4 D in diethyl ether, 5.7 D in tetrahydrofuran, 13 ± 2 D in *n*-butanol, 17 ± 4 D in acetonitrile, and 42 D in dimethyl sulfoxide. The μ_e value increased with solvent polarity except in benzene. The value of μ_e in benzene was exceptionally large despite of very low dielectric constant.

Rotational Diffusion Coefficients of CMPE in Polar Solvents. Rotational diffusion coefficients of CMPE determined from the anisotropy decays are also listed in Table 3, together with calculated diffusion coefficients considering both slip and stick models. In benzene, the observed D_0's were closer to the calculated D_0's with stick model, rather than those with slip model. In *n*-butanol D_0 (obs) was much higher than both D_0 (calc)'s at low temperatures, but quite close to D_0 (calc) with slip model at high temperatures. In dimethyl sulfoxide D_0 (obs) was quite close to D_0 (calc) with stick model. In diethyl ether, tetrahydrofuran and acetonitrile the values of D_0 (obs) were much smaller than those of D_0 (calc).

Stokes Shift in *n*-Propanol. Stokes shift of CMPE was shown in Figure 5. The observed data were analyzed by the present method. Frequency-dependent dielectric constant of *n*-propanol is described with three relaxation times. Parameters used for the analysis are listed in Table 4. Very fast decay was seen at the early stage in the calculated Stokes shift. The fast decay is reasonable in the theoretical Stokes shift because the dielectric constant contains very fast relaxation times of τ_2 and τ_3. It should be difficult to observe such fast decay by the excitation with our laser pulse (pulse width of response function, ca. 30 ps).

μ_e, μ_g, and D_0 were determined from these parameters by the method described in **Method of Analysis** section. The values of μ_e and μ_g were 9.5 and 0 D, respectively. This suggests that dipole moment of CMPE is very small in the ground state. The observed D_0 is quite close to the calculated one with slip model.

Simultaneous Analysis of Anisotropy Decay and Stokes Shift. Anisotropy decay and Stokes shift of CMPE in *n*-butanol are shown in Figures 6. The anisotropy decay was nonexponential, whereas those in other solvents were monoexponential. The nonexponential decay is expected when the rotational diffusion coefficient is in the same order as the Debye relaxation time.[19] Stokes shift decayed with almost monoexponential function in the time range examined. These decays were analyzed simultaneously. Both calculated decays fit well with the observed ones. The parameters used and obtained are listed in Table 5. The values of μ_e and μ_g were 14 and 1.5 D, respectively, in *n*-butanol. The dipole moment in the ground state was also small in *n*-butanol, as it was in *n*-propanol. Rotational diffusion coefficient was quite close to the one with slip model.

Transient Absorption Spectra of CMPE. Picosecond time-resolved absorption spectra of CMPE in *n*-hexane, acetonitrile and dioxane are shown in Figure 7. Change in the absorption spectra in these solvents at various delay times are shown in Figure 8. From the similarity of the transient absorption spectra of cyanodiphenylethyne at short delay times, the transient absorption band peaked around 505 nm in *n*-hexane can safely be assigned to the $S_n \leftarrow S_1$ transition of CMDE. Because the decay time of the 505-nm band was about 0.8 ns and was in good agreement with the rise time of the 460-nm band, the 460-nm band is ascribed to the $T_n \leftarrow T_1$ transition of CMDE. The band around 640 nm was also considered to be due to the S_1

TABLE 3: Parameters Used and Determined by the Analyses of Anisotropy Decays of CMPE[a]

								D_0/ns^{-1} (calc)	
solvent	T/°C	ϵ_0[b]	η[c]/mPas	τ_D[d]/ps	λ_{em}/nm	μ_e/D	D_0/ns^{-1} (obs)	slip	stick
benzene	6	2.31	0.896	5.5	360	9.73	1.17	2.55	1.23
					380	9.81	1.26		
	9	2.30	0.738	5.4	360	10.5	1.15	3.15	1.52
					380	10.2	1.14		
	14	2.29	0.707	5.3	360	9.91	1.47	3.35	1.61
					380	9.87	1.27		
	30	2.27	0.564	5.0	360	9.59	1.40	4.43	2.14
					390	9.39	1.50		
diethyl ether	22	4.3	0.24	2.4	360	3.4	2.74	10.1	4.89
					420	3.4	2.66		
tetrahydrofuran	22	7.6	0.50	4.0	360	5.7	1.88	4.87	2.35
					420	5.7	1.64		
n-butanol	4	20.0	4.6	1090	360	16	0.848	0.427	0.240
					370	12	1.058		
					420	12	0.842		
	9	19.3	3.98	905	370	12	0.856	0.584	0.282
					420	12	0.888		
	14	18.6	3.47	754	370	15	1.08	0.683	0.329
					420	11	0.880		
	22	17.6	2.80	573	360	14	0.754	0.869	0.419
					420	15	1.15		
	30	16.6	2.28	444	370	14	1.27	1.10	0.529
					420	8.2	0.777		
acetonitrile	4	39.6	0.416	4.13	370	12	1.53	5.49	2.65
					420	17	1.86		
	9	38.9	0.396	4.05	420	23	1.79	5.88	2.84
	14	38.0	0.376	3.98	370	15	1.83	6.29	3.03
					420	21	1.86		
	22	36.7	0.349	3.9	360	18	1.72	6.97	3.36
					420	17	2.24		
	30	35.4	0.325	3.77	370	9.7	2.55	7.69	3.71
					420	20	2.25		
dimethylsulfoxide	22	46.5	2.0	20.6	360	42	0.447	1.22	0.578
					420	41	0.572		

[a] μ_e was determined at certain value of D_0 which was sequentially varied at the intervals of 0.001 (ns^{-1}). [b] $\epsilon_0(T)$ at temperature T was evaluated assuming that it decreases proportionally to temperature. [c] Viscosity at T was evaluated by the following equation:[40] $\eta(T) = A \exp(B/RT)$. Constants, A and B were determined by a least-squares method when the viscosities are known at several temperatures. [d] Temperature dependences of Debye relaxation time were evaluated by the following equation:[41] $\tau(T) = A/T$. The value of A was determined when $\tau(T_0)$ at T_0 is known.

TABLE 4: Analysis of Stokes Shift of CMPE in *n*-Propanol[a]

								D_0/ns^{-1}	D_0/ns^{-1} (calc)	
η/mPas	ϵ_∞	ϵ_0	τ_1/ps (g_1)	τ_2/ps (g_2)	τ_3/ps (g_3)	μ_e/D	μ_g/D	(obs)	slip	stick
2.20	2.22	21.0	459 (0.923)	19.6 (0.034)	2.20 (0.043)	9.5	0.0	1.10	1.11	0.53

[a] Dielectric relaxation of *n*-propanol is represented with three-relaxation times. The g_1, g_2 and g_3 in eq 14 are expressed with ϵ_{0_i} and ϵ_{∞_i} (i = 1, 2, 3) given by Castner et al.,[24] as follows: $g_i = (\epsilon_{0_i} - \epsilon_{\infty_i})/(\epsilon_{01} - \epsilon_{\infty_3})$, ($i$ = 1,2,3). μ_e and μ_g was determined by the nonlinear least-squares's method at a certain value of D_0 which was varied sequentially at the intervals of 0.01 (ns^{-1}).

TABLE 5: Simultaneous Analysis of Anisotropy Decay and Stokes Shift of CMPE in *n*-Butanol[a]

							D_0/ns^{-1} (calc)	
ϵ_0	η/mPas	τ_D[b]/ps	μ_e/D	μ_g/D	A_0[c]	D_0/ns^{-1} (obs)	slip	stick
17.6	2.78	573	14	1.5	0.40	0.943	0.874	0.422

[a] μ_e, μ_g, θ_g were determined by the nonlinear least-squares method at a certain value of D_0 which was varied sequentially at the intervals of 0.001 (ns^{-1}). Emission was monitored at 420 nm for the anisotropy decay. Temperature was 22 °C. [b] The value of τ_D was taken from the data given by Castner et al.[24] [c] A_0 is limiting polarization anisotropy. θ_g is related to A_0 by the equation, $A_0 = 1/5(3\cos\theta_g - 1)$.

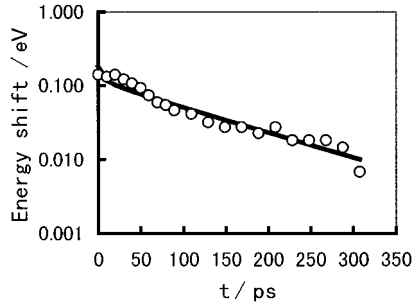

Figure 5. Time-Dependent Stokes shift of CMPE in *n*-propanol. Observed and calculated energy shifts are shown by open circles and solid curve, respectively. Parameters used and obtained are listed in Table 4.

state because no monitor wavelength dependence of the decay time was observed. Unlike diphenylethyne, the lowest excited singlet state of the diphenylethyne derivatives with cyano-group is the B_{1u} state which is dipole allowed from the ground state.[28] In acetonitrile immediately after the laser pulse excitation, the transient absorption band appeared at 460 nm, which was rapidly replaced by the broad absorption band peaked at the wavelengths

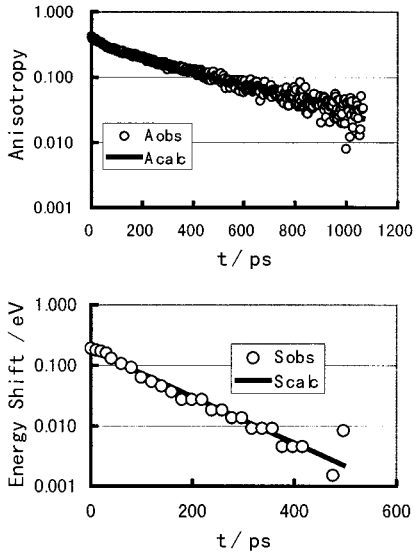

Figure 6. Simultaneous analysis of anisotropy decay and Stokes shift of CMPE in *n*-butanol. The anisotropy and Stokes shift were analyzed with common parameters, which are listed in Table 5.

of 605 nm and less than 430 nm. The rise time monitored at 605 nm was not instrumentally limited but it was less than 10 ps. The decay time measured at 605 nm in acetonitrile was estimated to be about 1 ns, which was in accord with fluorescence lifetime from the charge-separated state. Therefore, we can safely assign the 605-nm band to the charge separated state of CMDE in acetonitrile. The long-lived band peaked around 465 nm was due to the triplet state.

At the first glance, the band shape of the short-lived transient absorption in dioxane was similar to the $S_n \leftarrow S_1$ absorption of CMDE in *n*-hexane, but the spectral shape changed with increasing delay times even in the shorter than 100 ps region. The rise time of the transient absorption measured at 620 nm was about 20 ps and the similar time constant was obtained from the decay of short-lived component observed at 500 nm. The $T_n \leftarrow T_1$ band was observed at 460 nm in the delay times longer than 1 ns. The observed spectral change in the delay times of a few tens of picosecond should be due to the intramolecular charge transfer of CMDE. The rapidly decaying component at 500 nm was also observed in various polar solvents such as methanol, tetrahydrofuran, diethyl ether, and acetonitrile. The component in acetonitrile was very weak and its lifetime was less than 10 ps. The lifetime of the short-lived component was 10 ps in methanol. These results reveal that a charge separation in the excited singlet state of CMPE takes place in acetonitrile, methanol and dioxane within less than 10, 10, and 20 ps, respectively, after pulsed excitation. Similar process was also observed in 1,2-(*p*-cyano-*p*′-dimethylamino-diphenyl)-ethyne in various polar solvents.[29,30]

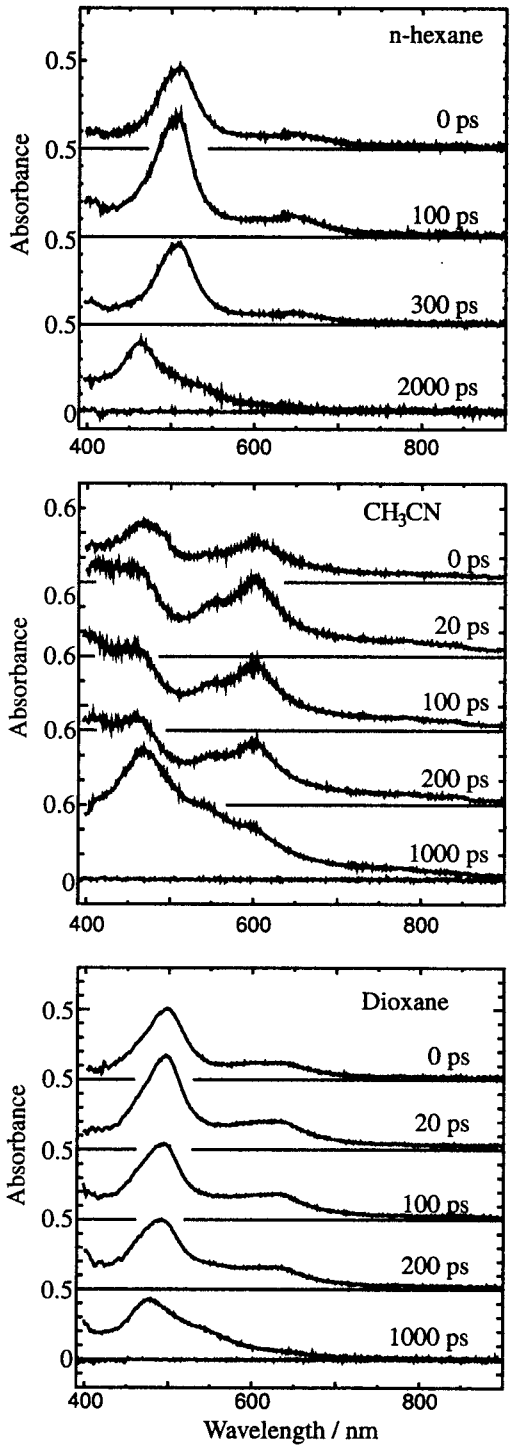

Figure 7. Picosecond time resolved absorption spectra of CMPE in *n*-hexane, acetonitrile and dioxane. Delay times after pulsed excitation are shown in the figure.

Discussion

Time-resolved fluorescence anisotropy and Stokes shift were analyzed with the unified theory based on continuum model.[19] In this theory, dielectric friction for the rotational motions of solute in polar solvents were introduced into the equations of both anisotropy decay and Stokes shift according to Nee and Zwanzig.[31] Measurements of anisotropy decays are useful to determine directly the dipole moment of solute molecules in the excited state. However, definite value of rotational diffusion coefficient is required to determine the dipole moment of the excited state. Anisotropy decay is sensitive to rotational diffusion coefficient of solute, and so the dipole moment depends much on the rotational diffusion coefficient used for the analysis. In most works,[6−15] on anisotropy decays of polar solute, the values of D_0 were calculated with various models including stick and slip models, and then contributions of dielectric friction on the reorientation motion of solute were evaluated. In the present work, we experimentally determined D_0 and μ_e, by which dielectric friction arises, so as to fit the calculated decays with the observed ones of anisotropy. The observed values of D_0 were compared with the calculated values of D_0 using stick and slip models.

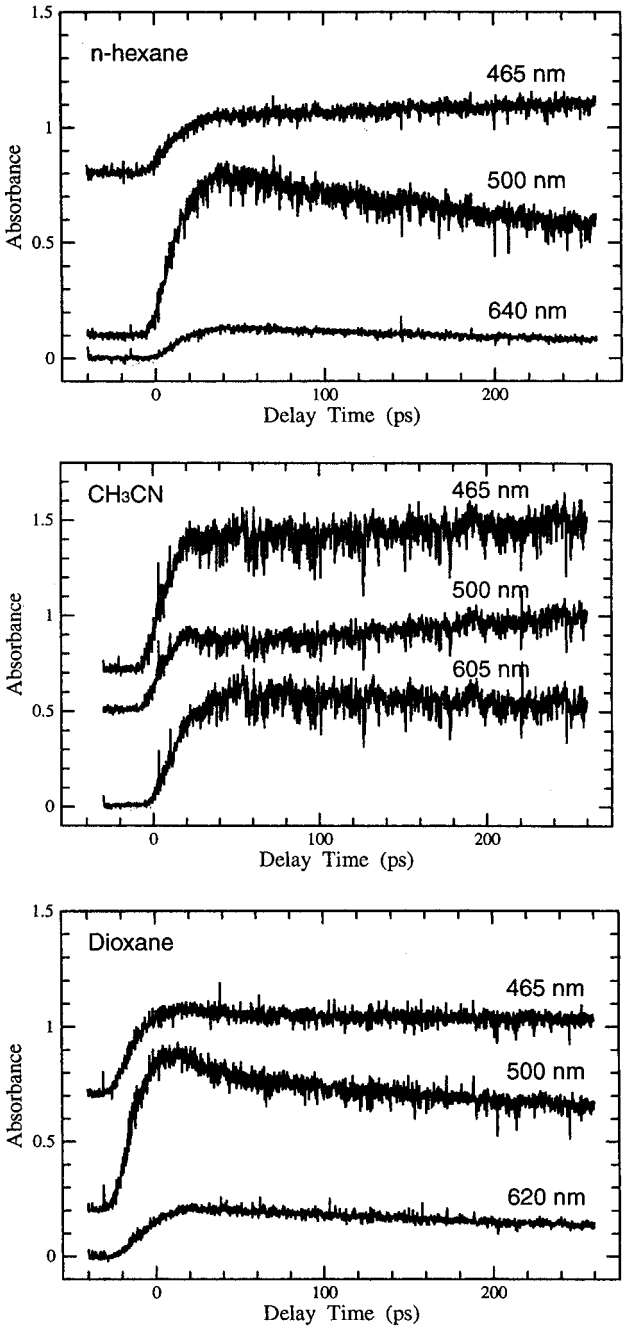

Figure 8. Changes in the Absorbance of Transient Absorption Spectra of CMPE in n-Hexane, acetonitrile and dioxane. Wavelengths monitored for absorbance are indicated beside the decay curves. Base lines of absorption curves are shifted upward for clearness.

Molecular structure of CMPE seems to be much simpler compared to aromatic dyes such as coumarine derivatives, phenoxazine derivatives and others used frequently for the studies of solvation dynamics. Directions of transition moment and dipole moments of CMPE are considered to be all along *z*-axis. Accordingly, the theoretical expressions[19] for anisotropy decay and Stokes shift can be applied to CMPE system. As shown in Table 3, the dipole moment of CMPE in the excited state depended on the solvent polarity. The results of transient absorption spectra of CMPE in a few solvents reveal that intramolecular CT states in the excited state of CMPE appeared in acetonitrile, methanol and dioxane within time less than 10, 10, and 20 ps, respectively, after pulsed excitation, whereas only the local excited-state did in *n*-hexane. Therefore, the time dependent fluorescence is considered to come from the LE state of the excited CMPE in nonpolar solvents and the CT state in polar solvents. The extent of the charge separation may be dependent on the solvent polarity.

It is important to point out that the dipole moment of the excited CMPE in benzene obtained in the present work was very large, despite of the very small dielectric constant. This result indicates a rather strong specific interaction between the excited solute dipole and solvent benzene. Such specific interaction between excited solute and "nonpolar" solvent benzene is considered to lead to the anomalously large fluorescence Stokes shift, which was already observed in the seminal works of fluorescence solvato-chronism by Mataga et al. in 1955.[32,33] Recently, it was also shown by the systematic investigations[34] on the photoinduced electron-transfer reactions of porphyrine-quinone dyads in various solvents of different polarities that the solvent reorganization energy to the excited dyads in benzene much larger than that expected from the classical Marcus equation.[35] This suggests also the strong specific interaction between the solvent benzene and porphyrin-quinone dyad undergoing the photoinduced electron-transfer reactions. The large solvent reorganization energy in benzene solution was interpreted by sophisticated theories[36] on the fundamental aspects of such solute−solvent interactions, or by quadrupole moment of benzene.[37]

Rotational diffusion coefficients of CMPE in 2,2,4-trimethylpentane and in *n*-pentadecane were reasonably described with stick and slip models, respectively, using half diameters of 0.82 nm for *z*-axis and 0.26 nm for *x*- or *y*-axis. In polar solvents with very short Debye relaxation time, diethyl ether, tetrahydrofuran, acetonitrile, the rotational diffusion coefficients were much smaller than those predicted with both models using these half diameters (see Table 3). In benzene with very short relaxation times, the diffusion coefficient was quite close to stick model at 6 °C, but much smaller than those predicted with both models at higher temperatures. In dimethyl sulfoxide with a relatively long relaxation time of 21 ps compared with above solvents, the diffusion coefficient was quite close but a little smaller than the one predicted with stick model. These results suggest that the rotation of the solute molecules accompanies with solvent molecules with the short relaxation times, so that the rotational motions become slowed.

Origin of the nonexponential behavior of the anisotropy decay in *n*-butanol is worth to discuss. Two reasons are conceivable, first, the effect of molecular shape of CMPE on the hydrodynamic reorientation, and, second, the effect of the frequency-dependent friction on the rotational motion of solute. The first possibility may be excluded because directions of the transition moments of absorption and emission are considered to be both along *z*-axis of CMPE. In fact the value of A_0 was 0.4, which shows the angle between both transition moments equal to zero. The second is realistic. In the previous work,[19] it was predicted that the anisotropy often decayed with nonexponential function when the frequency-dependent friction was introduced into rotational motion of solute. The nonexponential decay of anisotropy was also observed in the system of cresyl violet in *n*-dodecanol.[38] Although the origin of it was interpreted in terms of hydrodynamic reorientation of spheroid molecule, we believe that the frequency-dependent friction contributes in part to the nonexponential decay of cresyl violet.

Acknowledgment. We are grateful to Prof. Noboru Mataga for his critical discussions and review on the present work.

Appendix

The constants appeared in eq 15, A_j, B_l, a_j, and b_l ($j = 1$ to 4, and $l = 1$ to 3) may be obtained in the following way. Meaning of the other constants is described in text.

a_j is a root of the following fourth-order polynomial

$$f_1(x) = -P_3x^4 + \left[s^2D_zP_3 + \{r(r+1) - s^2\}D_0P_3 - \left(P_2 + \frac{R_2}{\zeta_0}F_3\right)\right]x^3 + \left[s^2D_z\left(P_2 + \frac{R_2}{\zeta_0}F_3\right) + \{r(r+1) - s^2\}D_0P_2 - \left(P_1 + \frac{R_1}{\zeta_0}F_3\right)\right]x^2 + \left[s^2D_z\left(P_1 + \frac{R_1}{\zeta_0}F_3\right) + \{r(r+1) - s^2\}D_0P_1 - \left(P_0 + \frac{R_0}{\zeta_0}F_3\right)\right]x + s^2D_z\left(P_0 + \frac{R_0}{\zeta_0}F_3\right) + \{r(r+1) - s^2\}D_0P_0 = 0 \quad \text{(A1)}$$

where

$$P_3 = \tau_1\tau_2\tau_3\{\epsilon_\infty + (\epsilon_c - \epsilon_\infty)A\} \quad \text{(A2)}$$

$$P_2 = (\tau_1\tau_2 + \tau_2\tau_3 + \tau_3\tau_1)\{\epsilon_\infty + (\epsilon_c - \epsilon_\infty)A\} + (1 - A)(\epsilon_0 - \epsilon_\infty)(g_1\tau_2\tau_3 + g_2\tau_3\tau_1 + g_3\tau_1\tau_2) \quad \text{(A3)}$$

$$P_1 = (\tau_1 + \tau_2 + \tau_3)\{\epsilon_\infty + (\epsilon_c - \epsilon_\infty)A\} + (1 - A)(\epsilon_0 - \epsilon_\infty)\{g_1(\tau_2 + \tau_3) + g_2(\tau_3 + \tau_1) + g_3(\tau_1 + \tau_2)\} \quad \text{(A4)}$$

$$P_0 = \epsilon_0 + (\epsilon_c - \epsilon_0)A \quad \text{(A5)}$$

A function, $h_1(x)$, is defined in eq A6

$$h_1(x) = -R_2x^3 - R_1x^2 - R_0x - 1 \quad \text{(A6)}$$

where

$$R_2 = \tau_1\tau_2\tau_3 \quad \text{(A7)}$$

$$R_1 = \tau_1\tau_2 + \tau_2\tau_3 + \tau_3\tau_1 - (g_1\tau_2\tau_3 + g_2\tau_3\tau_1 + g_3\tau_1\tau_2) \quad \text{(A8)}$$

$$R_0 = \tau_1 + \tau_2 + \tau_3 - \{g_1(\tau_2 + \tau_3) + g_2(\tau_3 + \tau_1) + g_3(\tau_1 + \tau_2)\} \quad \text{(A9)}$$

Then the coefficient A_j is obtained by eq A10

$$A_j = \frac{h_1(a_j)}{f_1'(a_j)} \quad \text{(A10)}$$

where $f_1'(a_j)$ is a differential coefficient of $f_1(x)$ in eq A1 at $x = a_j$.

b_1 is a root of the following third-order polynomial

$$f_2(x) = x^3 + E_2x^2 + E_1x + E_0 \quad \text{(A11)}$$

where

$$E_2 = \frac{1}{\{\epsilon_\infty + (\epsilon_c - \epsilon_\infty)A\}\tau_1\tau_2\tau_3}[\{\epsilon_\infty + (\epsilon_c - \epsilon_\infty)A\}\{g_1\tau_1(\tau_2 + \tau_3) + g_2\tau_2(\tau_3 + \tau_1) + g_3\tau_3(\tau_1 + \tau_2)\} + \{\epsilon_0 + (\epsilon_c - \epsilon_0)A\}(g_1\tau_2\tau_3 + g_2\tau_3\tau_1 + g_3\tau_1\tau_2)] \quad \text{(A12)}$$

$$E_1 = \frac{1}{\{\epsilon_\infty + (\epsilon_c - \epsilon_\infty)A\}\tau_1\tau_2\tau_3}[\{\epsilon_\infty + (\epsilon_c - \epsilon_\infty)A\}\{g_1\tau_1 + g_2\tau_2 + g_3\tau_3) + \{\epsilon_0 + (\epsilon_c - \epsilon_0)A\}\{g_1(\tau_2 + \tau_3) + g_2(\tau_3 + \tau_1) + g_3(\tau_1 + \tau_2)\}] \quad \text{(A13)}$$

$$E_0 = \frac{\epsilon_\infty + (\epsilon_c - \epsilon_\infty)A}{\epsilon_0 + (\epsilon_c - \epsilon_0)A} \cdot \frac{1}{\tau_1\tau_2\tau_3} \quad \text{(A14)}$$

As $h_1(x)$ in eq A6 we define $h_2(x)$ as eq A15

$$h_2(x) = T_2x^2 + T_1x + T_0 \quad \text{(A15)}$$

where

$$T_2 = \frac{-\epsilon_c(\epsilon_0 - \epsilon_\infty)(g_1\tau_2\tau_3 + g_2\tau_3\tau_1 + g_3\tau_1\tau_2)}{(\epsilon_c - \epsilon_\infty)\{\epsilon_\infty + (\epsilon_c - \epsilon_\infty)A\}\tau_1\tau_2\tau_3} \quad \text{(A16)}$$

$$T_1 = \frac{-\epsilon_c(\epsilon_0 - \epsilon_\infty)\{g_1(\tau_2 + \tau_3) + g_2(\tau_3 + \tau_1) + g_3(\tau_1 + \tau_2)\}}{(\epsilon_c - \epsilon_\infty)\{\epsilon_\infty + (\epsilon_c - \epsilon_\infty)A\}\tau_1\tau_2\tau_3} \quad \text{(A17)}$$

$$T_0 = \frac{-\epsilon_c(\epsilon_0 - \epsilon_\infty)}{(\epsilon_c - \epsilon_\infty)\{\epsilon_\infty + (\epsilon_c - \epsilon_\infty)A\}\tau_1\tau_2\tau_3} \quad \text{(A18)}$$

The coefficient, B_j, is obtained by eq A19

$$B_j = \frac{h_2(b_j)}{f_2'(b_j)} \quad \text{(A19)}$$

where $f_2'(b_j)$ is differential coefficient of $f_2(x)$ in eq A11 at $x = b_j$.

References and Notes

(1) Maroncelli, M.; McInnes, J; Fleming, G. R. *Science* **1989**, *247*, 1674.
(2) Barbara, P. F.; Jarzeba, W. *Adv. Photochem.* **1990**, *15*, 1.
(3) Mataga, N., Okada, T., Masuhara, H., Eds. *Dynamics and Mechanisms of Photoinduced Electron Transfer and Related Phenomena*; Elsevier: Amsterdam, 1992.
(4) Gauduel, Y., Rossky, P. J., Eds. *Ultrafast Reaction Dynamics and Solvent Effects*; AIP Press: New York, 1994.
(5) Fleming, G. R.; Cho, M. *Annu. Rev. Phys. Chem.* **1996**, *47*, 109.
(6) Kivelson, D.; Spears, K. G. *J. Phys. Chem.* **1985**, *89*, 1999.
(7) Philips, L. A.; Webb, S. P.; Clark, J. H. *J. Chem. Phys.* **1985**, *83*, 5810.
(8) Templeton, E. F. G.; Kenney-Wallace, G. A. *J. Phys. Chem.* **1986**, *90*, 5441.
(9) Simon, J. D.; Thomson, P. A. *J. Chem. Phys.* **1990**, *92*, 2891.
(10) Dutt, G. B.; Doraiswamy, S.; Periasamy, N.; Venkataraman, B. *J. Chem. Phys.* **1990**, *93*, 8498.
(11) Blanchard, G. J. *J. Phys. Chem.* **1991**, *95*, 5293.
(12) Alavi, D. S.; Waldeck, D. H. *J. Chem. Phys.* **1991**, *94*, 6196.
(13) Imeshev, G.; Khundkar, L. R. *J. Chem. Phys.* **1995**, *103*, 8322.
(14) Horng, M.-L.; Gardecki, J. A.; Maroncelli, M. *J. Phys. Chem. A* **1997**, *101*, 1030.
(15) Hartman, R. S.; Konitsky, W. M.; Waldeck, D. H.; Chang, Y. J.; Castner, E. W., Jr. *J. Chem. Phys.* **1997**, *106*, 7920.
(16) Shirota, H.; Castner, E. W., Jr. *J. Chem. Phys.* **2000**, *112*, 2367.
(17) Bagchi, B.; Oxtoby, D. W.; Fleming, G. R. *Chem. Phys.* **1984**, *86*, 257.

(18) van der Zwan, G.; Hynes, J. T. *J. Phys. Chem.* **1985**, *89*, 4181.
(19) Tanaka, F.; Mataga, N. *Chem. Phys.* **1998**, *236*, 288.
(20) Nomoto, T. *Bull. Fac. Educ. Mie University* **1986**, *37*, 9.
(21) Tamai, N.; Ishikawa, I.; Kitamura, N.; Masuhara, H. *Chem. Phys. Lett.* **1991**, *184*, 398.
(22) Hirata, Y.; Okada, T.; Mataga, N.; Nomoto, N. *J. Phys. Chem.* **1992**, *96*, 6559.
(23) Böttcher, C. J. F. *Theory of Electric Polarization* **1973** *Vol. 1*; Elsevier: Amsterdam.
(24) Castner, E. W., Jr.; Bagchi, B.; Maroncelli, M.; Webb, S. P.; Ruggiero, A. J.; Fleming, G. R. *Ber. Bunsen-Ges. Phys. Chem.* **1988**, *92*, 363.
(25) Perrin, F. *J. Phys. Radium.* **1934**, *7* (5), 497.
(26) Hu, C.-M.; Zwanzig, R. *J. Chem. Phys.* **1974**, *60*, 4354.
(27) Jiang, Y.; Blanchard, G. B. *J. Phys. Chem.* **1994**, *98*, 6436.
(28) Hirata, Y.; Okada, T.; Nomoto, T. *Chem. Phys. Lett.* **1993**, *209*. 397.
(29) Hirata, Y.; Okada, T.; Nomoto, T. *Chem. Phys. Lett.* **1997**, *278*, 133.
(30) Hirata, Y.; Okada, T.; Nomoto, T. *J. Phys. Chem.* **1998**, *102*, 6568.
(31) Nee, T.-W.; Zwanzig, R. *J. Chem. Phys.* **1970**, *52*, 6353.
(32) (a) Mataga, N., Kaifu, Y., Koizumi, M. *Bull. Chem. Soc. Jpn.* **1955**, *28*, 690. (b) Mataga, N., Kaifu, Y., Koizumi, M. *Bull. Chem. Soc. Jpn.* **1956**, *29*, 465.
(33) Lippert, E. (a) *Z. Naturforsh*. **1955**, *109*, 541. (b) *Ber. Bunsen-Ges. Phys. Chem*. **1957**, *61*, 962.
(34) Asahi, T.; Ohkohochi, M.; Matsusaka, R.; Mataga, N.; Zhang, R. P.; Osuka, A.; Maruyama, K. *J. Am. Chem. Soc.* **1993**, *115*, 5665.
(35) Marcus, R. A. *J. Chem. Phys.* **1956**, *24*, 966.
(36) Perng, B.-C.; Newton, M. D.; Raineri, F. O.; Friedman, H. L. (a) *J. Chem. Phys.* **1996**, *104*, 7153. (b) *J. Chem. Phys.* **1996**, *104*, 7177.
(37) Jeon, J.; Kim, H. J. *J. Phys. Chem. A* **2000**, *104*, 9812.
(38) Blanchard, G. J. *J. Chem. Phys.* **1987**, *87*, 6802.
(39) Dean, J. A. *Lange's Handbook of Chemistry*, 14th ed.; MaGraw-Hill, Inc.: New York, 1992.
(40) Barrow, G. M. *Physical Chemistry*, 3rd ed.; McGraw-Hill: New York, 1973.
(41) Daniel, V. V. *Dielectric Relaxation*; Academic Press: New York, 1967.